2002

Reduction Kinetics of Fe(III), Co(III), U(VI), Cr(VI), and Tc(VII) in Cultures of Dissimilatory Metal-Reducing Bacteria

Chongxuan Liu
Pacific Northwest National Laboratory, chongxuan.liu@pnl.gov

Yuri A. Gorby
Pacific Northwest National Laboratory

John M. Zachara
Pacific Northwest National Laboratory, john.zachara@pnl.gov

James K. Fredrickson
Pacific Northwest National Laboratory, jim.fredrickson@pnl.gov

Christopher F. Brown
Pacific Northwest National Laboratory

Reduction Kinetics of Fe(III), Co(III), U(VI), Cr(VI), and Tc(VII) in Cultures of Dissimilatory Metal-Reducing Bacteria

Chongxuan Liu, Yuri A. Gorby, John M. Zachara, Jim K. Fredrickson, Christopher F. Brown

Pacific Northwest National Laboratory, Richland, Washington 99352; telephone: (509) 376-0129; fax: (509) 376-3650; e-mail: chongxuan.liu@pnl.gov

Received 18 January 2002; accepted 23 May 2002

DOI: 10.1002/bit.10430

Abstract: The reduction kinetics of Fe(III)citrate, Fe(III)NTA, Co(III)EDTA$^-$, U(VI)O_2^{2+}, Cr(VI)O_4^{2-}, and Tc(VII)O_4^- were studied in cultures of dissimilatory metal reducing bacteria (DMRB): *Shewanella alga* strain BrY, *Shewanella putrefaciens* strain CN32, *Shewanella oneidensis* strain MR-1, and *Geobacter metallireducens* strain GS-15. Reduction rates were metal specific with the following rate trend: Fe(III)citrate $\geq$ Fe(III)NTA > Co(III)EDTA$^-$ $\gg$ UO_2^{2+} > CrO_4^{2-} > TcO_4^-, except for CrO_4^{2-} when H_2 was used as electron donor. The metal reduction rates were also electron donor dependent with faster rates observed for H_2 than lactate$^-$ for all *Shewanella* species despite higher initial lactate (10 m*M*) than H_2 (0.48 m*M*). The bioreduction of CrO_4^{2-} was anomalously slower compared to the other metals with H_2 as an electron donor relative to lactate and reduction ceased before all the CrO_4^{2-} had been reduced. Transmission electron microscopic (TEM) and energy-dispersive spectroscopic (EDS) analyses performed on selected solids at experiment termination found precipitates of reduced U and Tc in association with the outer cell membrane and in the periplasm of the bacteria. The kinetic rates of metal reduction were correlated with the precipitation of reduced metal phases and their causal relationship discussed. The experimental rate data were well described by a Monod kinetic expression with respect to the electron acceptor for all metals except CrO_4^{2-}, for which the Monod model had to be modified to account for incomplete reduction. However, the Monod models became statistically over-parametrized, resulting in large uncertainties of their parameters. A first-order approximation to the Monod model also effectively described the experimental results, but the rate coefficients exhibited far less uncertainty. The more precise rate coefficients of the first-order model provided a better means than the Monod parameters, to quantitatively compare the reduction rates between metals, electron donors, and DMRB species. © 2002 Wiley Periodicals, Inc. *Biotechnol Bioeng* **80:** 637–649, 2002.

Keywords: kinetics; metal; metal-reducing bacteria; bioreduction; biogenic precipitate

Contract grant sponsors: Natural and Accelerated Bioremediation Research Program (NABIR); Office of Biological and Environmental Research (OBER); U.S. Department of Energy (DOE)

Correspondence to: Chongxuan Lui, Pacific Northwest National Laboratory, P.O. Box 999, MSIN K8-96, Richland, WA 99352

INTRODUCTION

Dissimilatory metal reducing bacteria (DMRB) can reduce various metals and radionuclides, including sediment-abundant Fe(III) and Mn(III/IV) and aqueous species of U(VI), Cr(VI), Co(III), and Tc(VII) (Gorby et al., 1998; Gorby and Lovley, 1992; Lloyd and Macaskie, 1996; Lovley, 1993; Lovley et al., 1991; Nealson and Saffarini, 1994; Roden and Zachara, 1996; Wildung et al., 2000). It is well established that DMRB-facilitated reduction accounts for the majority of the valence transitions of Fe(III) to Fe(II) in anoxic, non-sulfidogenic, and low-temperature environments. The DMRB-mediated reduction is also an important process in controlling the fate and transport of hazardous metals and radionuclides in anoxic sediments, such as natural and engineered wetlands and contaminated subsurface environments. Because of their low solubility, the reduced forms of some contaminant metals and radionuclides (e.g., U, Cr, Tc) precipitate as immobile forms during microbial reduction process (De Luca et al., 2001; Fredrickson et al., 2001; Gorby and Lovley, 1992; Liu et al., 2001b; Lloyd et al., 2001; Lovley et al., 1991; Wildung et al., 2000). Hence, microbial reduction represents a potential strategy for the in-situ immobilization and containment of contaminant metals and radionuclides in aqueous waste streams and subsurface environments.

Although the importance of DMRB in controlling the fate and transport of metals and their potential for remediation purposes are well recognized, kinetic information on metal reduction is lacking and models of these enzymatic processes are scarce. DMRB reduce metals during anaerobic respiration through a cell membrane-associated electron transport system (ETS) (Aubert et al., 2000; Brock et al., 1994; Myers and Nealson, 1990). The ETS consists of various functional-specific enzymes and coenzymes that mediate intermediate and terminal redox processes and electron transport (e.g., Brock et al., 1994). The biochemical reactions controlling electron flux to the ETS from the electron donor, and their transport within the ETS determine the rate of electron transfer from electron donor to acceptor. The

macroscopic kinetics of metal reduction manifests the biochemical reactions and processes in such a networked system.

Mathematically, the kinetics of metal reduction can be described in two ways. The first is to systematically couple and solve all the networked biochemical reactions and processes in terms of experimentally measurable quantities and properties (Easterby, 1984, 1989; Moran et al., 1997; Vlad et al., 1999; Vlad and Ross, 2000). The analyses from such kinetic models provide detailed insights into the mechanisms of biochemical reactions and processes. However, due to the extremely complex biochemical nature of the ETS, a more macroscopic approach has often been used in describing the kinetics of microbial-mediated reactions. In this latter approach, the biochemical network is simply treated as a catalytic "species" without considering its internal structure. The kinetics is formulated as a catalytic interaction model, such as the Monod bacterium-based models (Gaudy and Gaudy, 1980; Monod, 1949; Rittmann and McCarty, 2001). Kinetic models with such treatment are mathematically simple and have been used in designing and controlling modern wastewater treatment plants (Rittmann and McCarty, 2001; Tchobanoglous and Burton, 1991), and in biogeochemical reactive transport codes (e.g., Rittmann and VanBriesen, 1996; Salvage et al., 1996; Steefel and Van Cappellen, 1998; Tebes-Stevens et al., 1998; Van Cappellen et al., 1993). Monod based models have also been used to quantitatively describe substrate concentrations in microbial ecology (Atlas, 1993).

Despite their success in the practical application, the Monod bacterial-based models are empirically based and suffer the disadvantage that the parameters are usually problem-specific and change with environmental conditions. Consequently, the Monod models have often been modified to describe experimental results under different conditions (Rittmann and McCarty, 2001; Segel, 1993; Simkins and Alexander, 1984). The application of these kinetic models to metal reduction, therefore, has to be individually examined with respect to the specificity of the metals and DMRB.

Here we report on the reduction kinetics of a suite of polyvalent metals by four different DMRB using either H_2 or lactate$^-$ as the electron donor. The central objectives were to test macroscopic kinetic models for describing microbial reduction of metals and to determine if systematic trends in bioreduction rate existed between the DMRB and polyvalent metals and causal biogeochemical factors. All experiments were performed under similar conditions to facilitate comparisons of the kinetic data. Monod-based kinetic models were used to describe the experimental results due to the lack of information regarding the detailed biochemical networks involved in microbial metal reduction.

MATERIALS AND METHODS

Cells and Culture Conditions

Three facultative bacteria (*Shewanella putrefaciens* strain CN32, *Shewanella alga* strain BrY, and *Shewanella oneidensis* strain MR-1) and a strict anaerobe (*Geobacter metallireducens* strain GS-15) were used as test organisms. These bacteria were isolated from anaerobic sediments and are commonly used in laboratory studies of metal reduction. *S. putrefaciens* strain CN32 was isolated from an anaerobic aquifer in northwestern New Mexico. *S. oneidensis* strain MR-1 was isolated from anaerobic sediments of Oneida Lake, New York, as a Mn(IV) reducer (Myers and Nealson, 1988). *S. alga* strain BrY was isolated from the Great Bay estuary in New Hampshire (Caccavo et al., 1992). The *Shewanella* strains were grown aerobically in 250-mL Erlenmeyer flasks with 100 mL of tryptic soy broth (TSB). Cultures were incubated for 16 h on a rotary shaker (100 rpm) at 30°C. Cells were harvested by centrifugation (5,500*g*, 15 min, 4°C), washed twice with 30 m*M* sodium bicarbonate (pH 6.8) that was made anoxic by bubbling with a N_2:CO_2 (80:20) gas mix, and suspended to a final concentration of about 2.5×10^9 cells/mL in an anoxic buffer containing 2 m*M* sodium bicarbonate. Cells were stored on ice and used within 4 h.

Geobacter metallireducens strain GS-15 was grown in a chemically defined medium (Lovley and Philips, 1988) with 50 m*M* Fe(III)citrate as the terminal electron acceptor and 50 m*M* sodium acetate as the electron donor. Cells were washed and stored as described above with the exception of precautions taken to prevent exposure of cells to air.

Chemicals

Aqueous species of Fe(III) [Fe(III)NTA and Fe(III)citrate], Co(III) [Co(III)EDTA$^-$], Cr(VI), U(VI), and Tc(VII) were used to study dissimilatory metal reduction. The aqueous Fe(III) was used to facilitate the rate comparison with other soluble metals to avoid the impacts of the reduction kinetics by oxide surface. A stock solution of Fe(III)NTA was prepared by dissolving 1.64 g $NaHCO_3$, 0.256 g of trisodium nitrilotriacetic acid (NTA), and 0.27 g of ferric dichloride in a water with a total volume of 100 mL. The solution was made anoxic by purging with O_2-free N_2:CO_2 (80:20) and stored in a sealed vial until needed. Fe(III)citrate and potassium chromate (K_2CrO_4) were obtained from Sigma Chemical Co. (St. Louis, MO). Co(III)EDTA$^-$ was prepared by the method of Dwyer et al. (1955). Uranyl chloride (UO_2Cl_2) and ammonium pertechnetate (NH_4TcO_4) were purchased from Amersham International (Buckinghamshire, U.K.).

Reduction Kinetic Assays

The soluble, oxidized metal or chelated metal complexes were diluted to 500 μM in 20 m*M* sodium bicarbonate buffer (pH 6.8) containing 10 m*M* of either sodium lactate or sodium acetate as the electron donor. In selected systems, variable metal concentrations were used from 10 μM to 22.5 m*M*. The reaction mixtures (10 mL) were added to glass pressure tubes (26.3 mL) and made anoxic by bub-

bling for 10 min with N_2:CO_2 (80:20). The calculated total carbonate concentrations equilibrated with the gas mixture was about 26 m*M* at pH 6.8 using MINTEQA2 code (Allison et al., 1991) with a thermodynamic database compiled by the authors. The tubes were sealed with thick butyl rubber stoppers and aluminum crimp seals. Washed cells (approximately 1 mL) were added into anoxic reaction mixtures (2×10^8 cells/mL final concentration) through the rubber stoppers using needles and syringes that were made anoxic by sparging with N_2:CO_2. The effects of electron donor on the reduction kinetics were evaluated in select mixtures with 10 mL (about 0.41 mmol) of H_2 instead of lactate. After partitioning between aqueous and gas phase, the aqueous H_2 concentration was bout 0.48 mmol/L calculated using the Henry's constant (H) of 7.03×10^4 atm in water ($H = P/X$, where P is partial pressure, and X is aqueous molar fraction). The H_2 gas was charged to sealed vials through the rubber stopper using a needle and syringe. The total concentrations of the electron donors were in stoichiometric excess with respect to electron equivalents needed for polyvalent metal reduction.

At selected time points, samples were taken using degassed needles and syringes and assayed for metal reduction. The reduction of Fe(III)NTA and Fe(III)citrate was monitored by measuring Fe(II) using the Ferrozine method (Lovley and Philips, 1987). The loss of CrO_4^{2-} was followed using the diphenyl carbazide colorimetric assay (Lloyd and Macaskie, 1996). Co(III)$EDTA^-$ and Co(II)$EDTA^{2-}$ were quantified by ion chromatography using the method described in (Jardine and Taylor, 1995). The reduction of UO_2^{2+} was monitored using a Kinetic Phosphorescence Analyzer (Chemcheck, Inc., Richland, WA) as described previously (Gorby and Lovley, 1992). The reduction of technetium was evaluated by determining pertechnetate in solution through direct extraction (Tribalat and Beydon, 1953) and liquid scintillation counting of ^{99}Tc (0.292 MeV beta) (Wildung et al., 2000).

Transmission Electron Microscopy (TEM)

TEM samples were prepared in an anaerobic glove box to avoid oxidation of reduced products. Cell suspensions were washed 3 times with 0.1 *M* Na cacodylate buffer at pH 7.2 followed by 3 washes with cold deionized water. The cells were gently pelleted, fixed in glutaraldehyde, dehydrated by EtOH wash, and embedded in LR White resin. The polymerized blocks were anaerobically sectioned on a microtome, and thin sections were mounted on copper grids coated with Formvar and carbon. The samples were not stained and were examined with an acceleration voltage of 200 kV on a JEOL 2010 TEM using the smallest possible apertures. The elemental composition of cell-associated precipitates was determined using energy-dispersive spectroscopy (EDS) (Oxford Instruments).

Kinetic Models

Monod-based kinetic models have the following basic formulation:

$$\frac{dS}{dt} = -\frac{(\mu_{max}/Y)X}{K_s + S} S, \quad (1)$$

$$\frac{dX}{dt} = -Y\frac{dS}{dt}, \quad (2)$$

where S is the substrate concentration, X is the bacterium concentration, μ_{max} is the maximum specific growth rate, K_s is the half-velocity constant, Y is the biomass yield per substrate loss, and t is the time. Although the kinetic model described by Eqs. (1) and (2) was originally derived for the electron donor (Gaudy and Gaudy, 1980; Monod, 1949; Rittmann and McCarty, 2001), it may also be used for electron acceptors when the kinetic rate is limited by the electron acceptor and when the concentration of electron donor is in excess (e.g., Bae and Rittmann, 1996; Liu et al., 2001c; Rittmann and VanBriesen, 1996; Spear et al., 1999; Wang and Shen, 1997). A constant growth yield (Y) is often assumed in modeling the microbial growth (Gaudy and Gaudy, 1980; Rittmann and McCarty, 2001). For DMRB with respect to Fe(III)citrate reduction, a constant yield of about 5×10^9 cells/mmol of electron transfer was previously observed under various reduction conditions (Liu et al., 2001c).

Assuming that Y is constant during the course of metal reduction, Eq. (2) can be integrated as

$$X = X_0 + Y(S_0 - S), \quad (3)$$

where X_0 and S_0 are the initial cell and substrate concentrations, respectively. When the initial cell concentration (X_0) is $\geqslant YS_0$, the effect of bacterial growth on the substrate degradation (Eq. (1)) can be neglected. For the analysis that follows, we neglected cell growth (Eq. (2)) in the Monod model because a high initial cell concentration (2×10^8 cells/mL) was used and growth-supporting nutrients were not provided. We also assumed that the cell decay was neglected because of relative short experimental durations and high initial cell concentrations. Otherwise, the cell growth model (Eq. (2) or (3)) has to be modified by a decay term. When $X = X_0$, the Monod model (Eq. (1)) has the same form as the Michaelis–Menten expression:

$$\frac{dS}{dt} = -\frac{V_m}{K_s + S} S, \quad (4)$$

where V_m equals $(\mu_{max}/Y)X_0$ in Eq. (1).

The Monod/Michaelis–Menten models as described by Eq. (4) apply when the byproducts of the biogeochemical reaction have no effects on the activity of the bacteria. If the reduction products inhibit cell activity, e.g., Cr(III) (Wang and Shen, 1997; Wang and Xiao, 1995; Wielinga et al., 2001), Eq. (1) has to be modified to incorporate inhibition effects. Various modifications have been proposed for the

Monod expression to account for the toxicity effects of substrates or products depending on mechanistic assumptions (Roels, 1983; Segel, 1993). On the basis of the detailed studies of microbial reduction of Cr(VI) inhibited by product Cr(III) (Wang and Shen, 1997; Wang and Xiao, 1995), Wang and Shen (1997) proposed a modified Monod model with the active cell concentration (X), expressed by

$$X = (X_0 - R_i(S_0 - S)), \quad (5)$$

where R_i is the inhibition coefficient. Eq. (5) assumes that the active cell concentration decreases with increasing reduction product formation. The microbial reduction of Cr(VI) could be well described by a combination of Eqs. (1) and (5) (Wang and Shen, 1997). Eq. (5) allows definition of the maximum reducible substrate concentration (X_0/R_i) that occurs when $X = 0$. This variable was denoted as R_m ($= X_0/R_i$) in the analysis that follows. In the case where the reaction (reduction) products do not inhibit microbiologic activity, R_i is zero and $R_m = \infty$. A modified version of Eq. (1) that incorporates R_m is

$$\frac{dS}{dt} = -\frac{V_m S}{K_s + S}(1 - (S_0 - S)/R_m). \quad (6)$$

A disadvantage in using the Monod model (Eq. (1)) is that the parameters of K_s and V_m are highly correlated under many experimental conditions (Liu and Zachara, 2001; Robinson, 1985). As a result of high correlation, the estimated parameters are extremely sensitive to experimental error and, thus, can contain large uncertainties (Liu and Zachara, 2001). A statistical analysis for Eq. (4) indicated that the uncertainties in K_s and V_m depend on the ratio of S_0/K_s, and that high uncertainties in K_s and V_m occur at a low ratio of S_0/K_s (<1) (Liu and Zachara, 2001). We have performed similar statistical analysis for the modified Monod rate expression (Eq. (6)) regarding the uncertainties in K_s, V_m, and R_m using the method developed in Liu and Zachara (2001) (results not shown here). The analysis indicated that the uncertainties of K_s, V_m, and R_m are primarily dependent upon two dimensionless variables: S_0/K_s and R_m/S_0 with the higher uncertainties in K_s, V_m, and R_m at a low ratio of S_0/K_s (<10) and at a high ratio of R_m/S_0 (>1).

K_s and V_m (and R_m for Eq. (6)) with high uncertainty are unreliable and preclude credible comparisons of experimental results obtained with different bacteria, electron acceptors, and donors because small differences of measurement errors will lead to large changes in values of the estimated parameters. Careful manipulation of the initial substrate concentrations can reduce correlations, thereby producing better estimates of K_s and V_m (Liu and Zachara, 2001). However, ideal experimental conditions are difficult to achieve because K_s, and R_m for Eq. (6), are unknown before performing the experiments to estimate them. An iterative experimental and parameter estimation approach was previously proposed (Liu and Zachara, 2001). This approach involves several iterations and may lead to the requirement of unrealistically high initial metal concentrations (S_0) that exceed solubility limitations and/or are environmentally unrealistic. For example, in order to meet the optimal experimental condition of $S_0/K_s = 5$–20 (Liu and Zachara, 2001) for bacterial reduction of Fe(III)citrate by CN32, the initial Fe(III)citrate concentration should be 145–580 mM based on an estimated K_s value of 29 mM (Liu et al., 2001c).

Because of these difficulties with parameter uncertainty, we have used the Monod model and its first-order approximation (Table I) to describe the bioreduction kinetic data. In the next section, we will show that both models effectively described the bioreduction kinetics of the metals by DMRB. However, the first-order approximation of the Monod model yielded estimated rate coefficients that had much higher precision, and accordingly, the first-order rate coefficients were used to quantitatively compare metal reduction rates for the different metals, electron donors, and DMRB species.

RESULTS

Bioreduction Kinetics

All *Shewanella* species used in this study were able to reduce Fe(III)citrate, Fe(III)NTA, Co(III)EDTA$^-$, U(VI)O_2^{2+}, and Cr(VI)O_4^{2-} (Figs. 1–5). GS-15 was also able to reduce all metals except for Cr(VI)O_4^{2-}. The reduction rates and extents, however, were different with respect to electron donors, metals, and DMRB species. With the exception of CrO_4^{2-}, all other metals studied were quantitatively reduced by the DMRB and the metal reduction rates were consistently faster using H_2 than lactate$^-$ as an electron donor for all *Shewanella* species and metals despite higher initial lactate (10 mM) concentration than H_2 (0.48 mM). A faster rate with H_2 relative to lactate$^-$ was also observed for the reduction of TcO_4^- by CN32 (Fig. 6). The behavior of CrO_4^{2-} was anomalous. It was completely reduced by CN32, but not by BrY or MR-1 within the experimental duration (Fig. 5a), and the reduction rate was slower with H_2 compared to lactate$^-$ as the electron donor (Fig. 5b).

The metal reduction rates by GS-15 were consistently slower than by the various *Shewanella* species for all studied metals. Among the *Shewanella* species studied, there was a trend that *S. putrefaciens* strain CN32 had the slowest reduction rates for all metals except CrO_4^{2-} regardless of whether the electron donor was H_2 or lactate$^-$, but the rate differences in cases of Fe(III) reduction with H_2 as the electron donor were generally small (Figs. 1 and 2). When lactate$^-$ was used as the electron donor, the trend of reduction rates for the *Shewanella* species was MR-1 > BrY > CN32. When H_2 was used as electron donor, the trend was BrY > MR-1 > CN32. However, the extent and rate of CrO_4^{2-} reduction by CN32 was greater and faster than it was for BrY and MR-1 (Fig. 5a).

Both the Monod and the first-order models were able to describe the experimental results (Figs. 1–6). The fitted results by both models were almost identical, and the figures

TABLE I. Summary of Monod model and its derivatives under no-growth condition.

Model and characteristics	Equations and inequalities
I Monod:	
Differential form	$dS/dt = -V_m S/(K_s + S)$
Integral form	$K_s \ln(S/S_0) + S - S_0 = -V_m t$
Derived parameter	$V_m = \mu_{max} X_0/Y$
Necessary condition	no growth and decay
II First-order:	
Differential form	$dS/dt = -k_1 S$
Integral form	$S = S_0 \exp(-k_1 t)$
Derived parameter	$k_1 = \mu_{max} X_0/(K_s Y)$
Necessary condition	$K_s \gg S_0$ and no growth and decay
III Monod, toxicity:	
Differential form	$dS/dt = -V_m S(1 - (S_0 - S)/R_m)/(K_s + S)$
Integral form	$K_s \ln(S_0/S) + (K_s + S_0 - R_m) \ln((R_m - S_0 + S)/R_m) = -V_m(S_0 - R_m)t/R_m$ for $R_m \neq S_0$
	or
	$\ln(S/S_0) + K_s(1/S_0 - 1/S) = -(V_m/S_0)t$ for $R_m = S_0$
Derived parameter	$V_m = \mu_{max} X_0/Y$
Necessary condition	$R_m \geq S_0 - S$ and no growth and decay
IV First-order, toxicity	
Differential form	$dS/dt = -k_1 S(1 - (S_0 - S)/R_m$
Integral form	$S = (S_0 - R_m)/(1 - (R_m/S_0) \exp(-k_1(S_0 - R_m)t/R_m))$ for $R_m \neq S_0$
	or
	$S = S_0/(1 + kt)$ for $R_m = S_0$
Derived parameter	$k_1 = \mu_{max} X_0/(K_s Y)$
Necessary condition	$R_m \geq S_0 - S$, $K_s \gg S_0$, and no growth and decay

show only the first-order model fit. A constant cell concentration (X_0) was used in fitting the total measured concentrations of Fe(III)citrate, Fe(III)NTA, Co(III)EDTA$^-$, $U(VI)O_2^{2+}$, and $Tc(VII)O_4^-$ using both models. Eq. (5) was used to describe active cell concentrations in the CrO_4^{2-} experiments to account for the incomplete reduction of Cr(VI). Both the Monod and first-order models had coefficients of determination (R^2) close to 1 in all cases (Table II), indicating that the model fits were good and comparable for either model. However, the estimated parameters from the first-order model were much more reliable due to their smaller standard deviations (Table II). In many cases, the standard deviations for the Monod parameters were larger than the parameter values themselves. The high uncertainties of K_s and V_m correlated with the small ratios of S_0/K_s ($\ll 1$) (Table II). As shown theoretically in a previous study (Liu and Zachara, 2001), the condition of $S_0/K_s \ll 1$ can result in significant errors in K_s and V_m estimation. In these cases, the Monod model degenerated into a first-order model as shown by the fact that the estimated ratio of V_m/K_s was close to the estimated first-order rate coefficient, k_1.

The first-order rate coefficients showed distinct trends with respect to organism, metal, and electron donor (Fig. 7). Such distinct trends cannot be provided by the Monod rate parameters due to their high uncertainties (Table II). The metal reduction rates followed the order (Fig. 7) Fe(III)citrate $\geq$ Fe(III)NTA > Co(III)EDTA$^-$ $\gg$ $U(VI)O_2^{2+}$ > $Cr(VI)O_4^{2-}$ > $Tc(VII)O_4^-$ for all studied cases, except for CrO_4^{2-} with H_2 as electron donor (Fig. 5b). The reduction

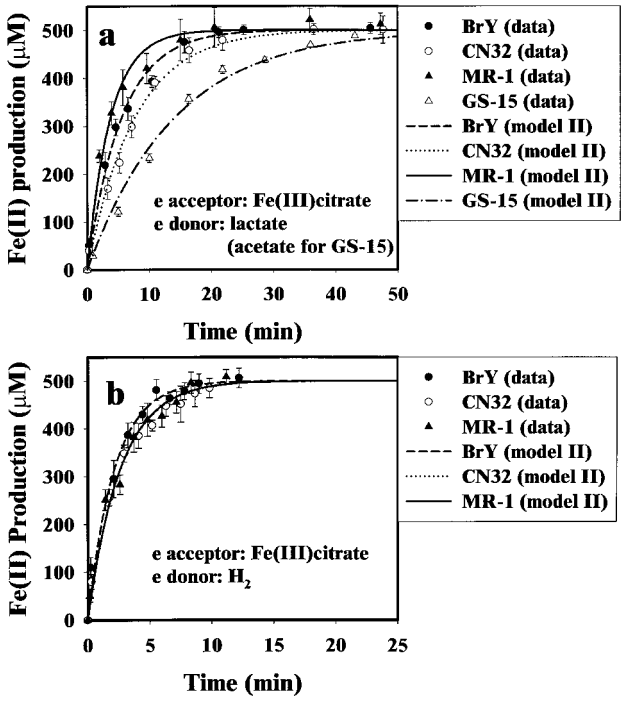

Figure 1. Experimental and first-order modeling results for Fe(III)citrate reduction (showing Fe(II) production) by different DMRB with lactate$^-$ (acetate$^-$ for GS-15) and H_2 as electron donors. The error bar represents one standard deviation of 3 replicates. The first-order model is described in Table I as model II.

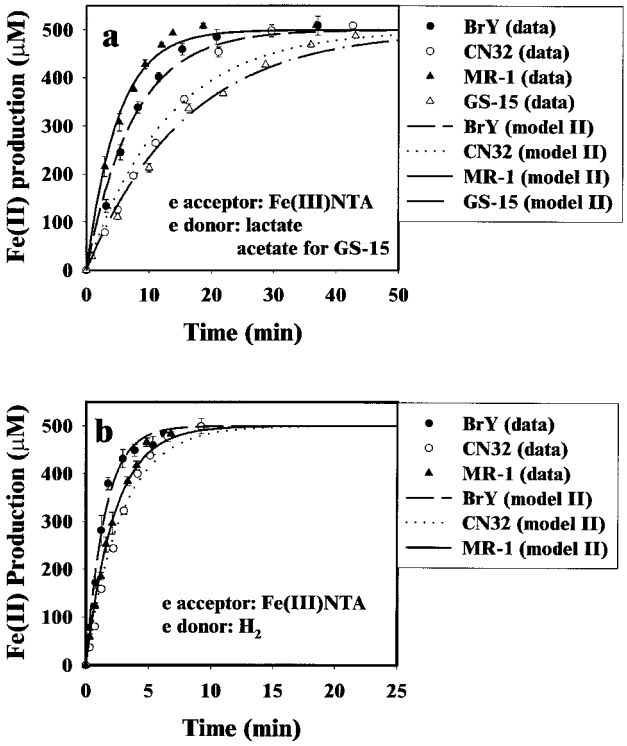

Figure 2. Experimental and first-order modeling results for Fe(III)NTA reduction (showing Fe(II) production). Other conditions are comparable to Fig. 1.

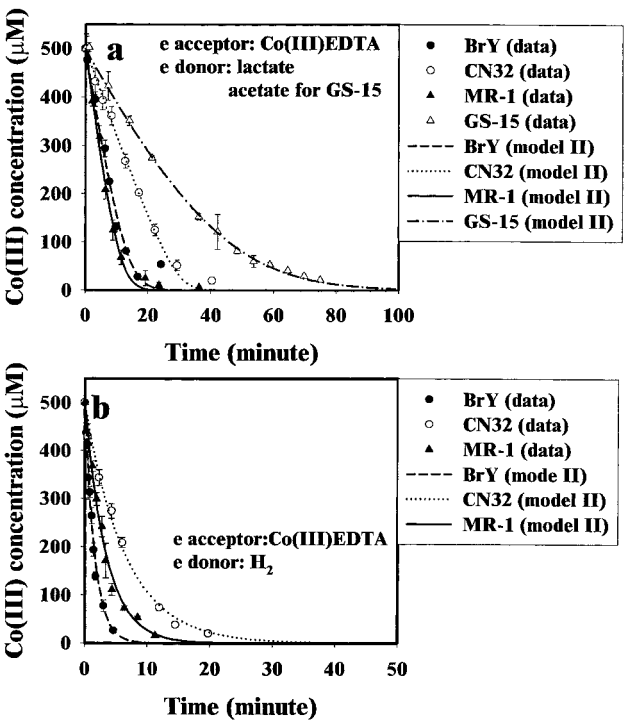

Figure 3. Experimental and first-order modeling results for Co(III)EDTA$^-$ reduction by different DMRB with lactate$^-$ (acetate$^-$ for GS-15) and H_2 as electron donors. The error bar represents one standard deviation of 3 replicates. The first-order model is described in Table I as model II.

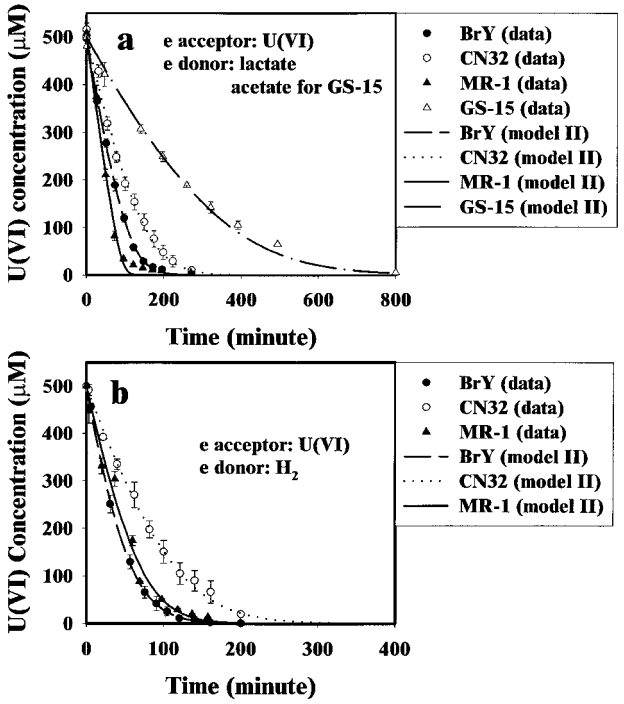

Figure 4. Experimental and first-order modeling results for U(VI)O_2^{2+} reduction. Other conditions are the same as in Fig. 3.

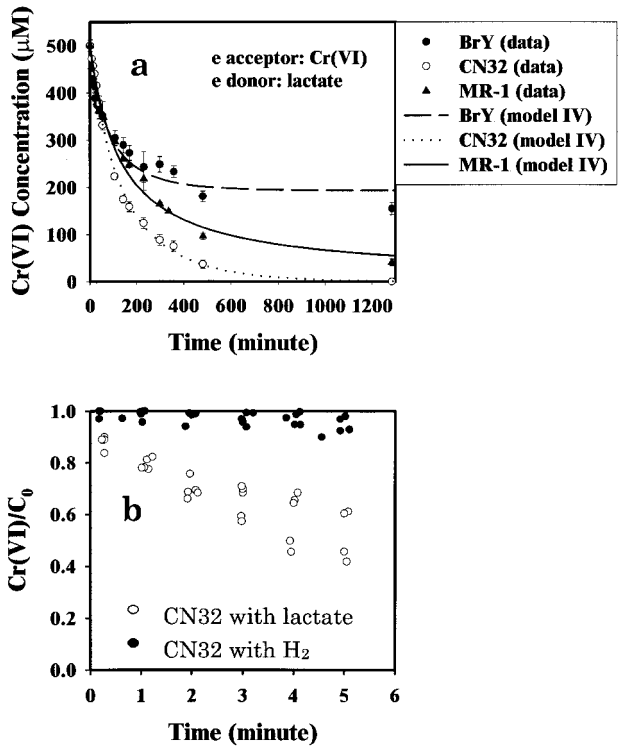

Figure 5. Experimental and first-order modeling results for Cr(VI)O_4^{2-} reduction by *Shewanella* species. (a) CrO_4^{2-} reduction with lactate$^-$ as electron donor (the error bar represents one standard deviation from 3 replicates; model IV is described in Table I). (b) Comparative bioreduction of CrO_4^{2-} by CN32 with lactate$^-$ and H_2 as electron donor normalized to initial concentration.

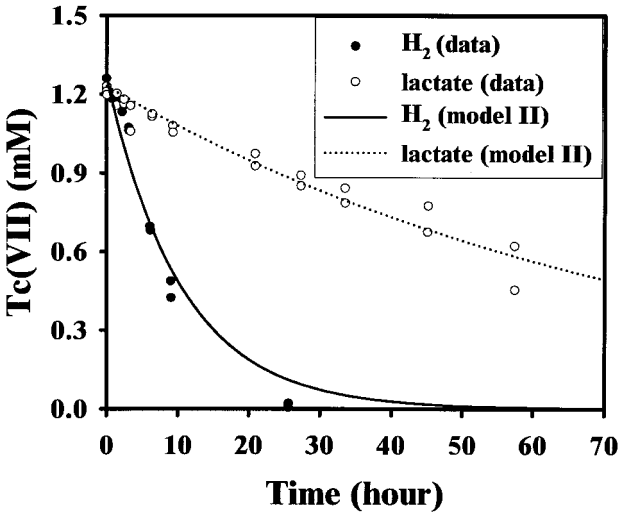

Figure 6. $Tc(VII)O_4^-$ reduction by CN32 using lactate$^-$ and H_2 as electron donors. Lines are first-order modeling results (model II in Table I).

rates of $U(VI)O_2^{2+}$, $Cr(VI)O_4^{2-}$, and $Tc(VII)O_4^-$ were much slower than organically complexed Fe(III) and Co(III) (Fig. 7). Except for CrO_4^{2-}, the rates of metal reduction using H_2 were approximately double the rates using lactate$^-$ as electron donor.

Reduction Thermodynamics and Cell-Associated Metal Reduction Products

The rates of bioreduction in Fig. 7 and Table II were not correlated with the overall free energy available for the biological reduction reactions as summarized in Table III. Lactate$^-$ was energetically comparable with H_2 as electron donors in terms of standard free energy changes (Fig. 8a) or more favorable in terms of reaction free energy changes (Fig. 8b) calculated using species concentrations correspondent to 10% of electron acceptor reduced according to the stoichiometric reactions (Table III), but H_2 generally yielded faster rates. Thermodynamically, $Cr(VI)O_4^{2-}$ was the preferred electron acceptors (e.g., $-\Delta G_r^{o'}$ and ΔG_r in Fig. 8a and b) as it was the strongest oxidants of the metals studied. This metal, however, along with $U(VI)O_2^{2+}$ and $Tc(VII)O_4^-$ consistently exhibited the slowest bioreduction rates. The three complexed metals were thermodynamically comparable in reaction free energies but were reduced at different rates. Acetate was less thermodynamically favorable as an electron donor than were lactate$^-$ or H_2 (Fig. 8). It is not known whether the slower rate of metal bioreduction by GS-15 relative to the *Shewanella* species was a result of this energy effect or physiologic or other biochemical reasons.

Unstained TEM images of cell thin sections of CN32 showed that U(IV) and Tc(IV) reduction products were associated with the outer membrane and periplasmic regions of the cells and in the case of U, fine-grained extracellular U precipitates were also observed (Fig. 9a,b). Similarly, U(IV) precipitates were also observed in association GS-15 cells although less extracellular U was observed compared to CN32 (Fig. 9c). These observations were consistent with previous reports of bioprecipitated $UO_{2(s)}$ and $TcO_{2(s)}$ (Fredrickson et al., 2001; Liu et al., 2001b; Lloyd et al., 2001; Wildung et al., 2000). In similar manner, $Cr(OH)_{3(s)}$ precipitates were also observed on the cell surface when Cr(VI) was reduced by CN32 and MR-1 (Y. A. Gorby, unpublished results). In contrast, no cell-associated precipitates were observed when Fe(III)citrate was reduced by CN32 (Liu et al., 2001c).

The results indicated that metals that precipitate as insoluble phases (e.g., Tc(IV), U(IV), Cr(III)) in their lower valence state, are bioreduced more slowly than those that do not precipitate or remain soluble as aqueous complexes (e.g., Fe(II)citrate$^-$, Fe(II)NTA$^-$) (Table IV). TEM analyses were not conducted of DMRB from the Co(III)EDTA$^-$, Fe(III)NTA reduction experiments, but it is predicted that the bioreduction products of Co(III)EDTA$^-$ or Fe(III)NTA reduction would remain soluble as aqueous complexes (Co(II)EDTA^{2-} and Fe(II)NTA$^-$) (Table IV).

DISCUSSION

Kinetic Models for Microbial Reduction of Metals by DMRB

Various modified Monod models have been proposed to describe the temporal dynamics of substrate degradation by microorganisms (Simkins and Alexander, 1984). Our results showed that a first-order model derived from the Monod model could describe the bioreduction of all metals in the absence of cell growth (Figs. 1–6). Although the overall kinetic model for Cr(VI) reduction (Model IV in Table I) was a mixed first- and second-order one with respect to the substrate concentration, the second-order component resulted from the necessity of modifying the active cell concentration by Eq. (5). The first-order approximation to the Monod model requires that $K_s \gg S_0$ (Table I), so that the denominator in Eq. (1) can be approximated by a constant value of K_s. This condition was satisfied for most cases of Fe(III)citrate, Fe(III)NTA, and CrO_4^{2-} reduction (Table I). The other cases generally exhibited conditions of $S_0/K_s < 2$ (Table I). This condition resulted in a linear correlation between K_s and V_m (Liu and Zachara, 2001). This linear correlation was exploited in fitting the experimental data by increasing the values of K_s and V_m with a fixed ratio of V_m/K_s. A large value of K_s will lead to the required first-order approximation condition of $K_s \gg S_0$. The first-order model can be a good approximation to Monod model for field conditions where the relevant contaminant metal concentrations ($\sim 10^{-6}$ M) $\ll K_s$, based on the estimated K_s values (Table II).

The large estimated standard deviations for K_s and V_m in Table II demonstrate that significant uncertainties propagate in the Monod model when $S_0/K_s < 1$, despite the good fit to

TABLE II. Summary of estimated kinetic parameters for metal reduction by DMRB.[a]

Metal	Bacterium	Electron donor	First-order model[b]	Monod model[b]
Fe(III)citrate	BrY	Lactate	$k_1 = 1.82\ (0.10) \times 10^{-1}$, $R^2 = 0.99$	$V_m = 1.54\ (90.5) \times 10^4$, $K_s = 8.45\ (498) \times 10^4$, $R^2 = 0.99$
		H_2	$k_1 = 4.62\ (0.330) \times 10^{-1}$, $R^2 = 0.98$	$V_m = 3.62\ (318) \times 10^4$, $K_s = 7.79\ (685) \times 10^4$, $R^2 = 0.99$
	CN32	Lactate	$k_1 = 1.32\ (0.06) \times 10^{-1}$, $R^2 = 0.99$	$V_m = 1.31\ (0.44) \times 10^2$, $K_s = 7.00\ (3.38) \times 10^2$, $R^2 = 1.00$
		H_2	$k_1 = 3.75\ (0.16) \times 10^{-1}$, $R^2 = 0.99$	$V_m = 3.02\ (149) \times 10^4$, $K_s = 8.00\ (396) \times 10^4$, $R^2 = 0.99$
	MR-1	Lactate	$k_1 = 2.69\ (0.19) \times 10^{-1}$, $R^2 = 0.99$	$V_m = 2.36\ (218) \times 10^4$, $K_s = 8.72\ (809) \times 10^4$, $R^2 = 0.99$
		H_2	$k_1 = 3.81\ (0.23) \times 10^{-1}$, $R^2 = 0.99$	$V_m = 3.09\ (223) \times 10^4$, $K_s = 8.00\ (578) \times 10^4$, $R^2 = 0.99$
	GS-15	Acetate	$k_1 = 7.16\ (0.32) \times 10^{-2}$, $R^2 = 0.99$	$V_m = 5.34\ (1.31) \times 10^1$, $K_s = 4.51\ (1.77) \times 10^2$, $R^2 = 1.00$
Fe(III)NTA	BrY	Lactate	$k_1 = 1.33\ (0.07) \times 10^{-1}$, $R^2 = 0.99$	$V_m = 7.51\ (1.28) \times 10^1$, $K_s = 2.63\ (0.92) \times 10^2$, $R^2 = 1.00$
		H_2	$k_1 = 6.55\ (0.34) \times 10^{-1}$, $R^2 = 0.99$	$V_m = 2.32\ (55.1) \times 10^3$, $K_s = 3.21\ (83.6) \times 10^3$, $R^2 = 0.99$
	CN32	Lactate	$k_1 = 7.82\ (0.64) \times 10^{-2}$, $R^2 = 0.97$	$V_m = 2.88\ (0.17) \times 10^1$, $K_s = 6.61\ (1.99) \times 10^1$, $R^2 = 1.00$
		H_2	$k_1 = 3.48\ (0.18) \times 10^{-1}$, $R^2 = 0.99$	$V_m = 1.71\ (0.17) \times 10^2$, $K_s = 1.90\ (0.45) \times 10^2$, $R^2 = 1.00$
	MR-1	Lactate	$k_1 = 2.00\ (0.08) \times 10^{-1}$, $R^2 = 0.99$	$V_m = 1.63\ (0.56) \times 10^2$, $K_s = 5.47\ (2.78) \times 10^2$, $R^2 = 1.00$
		H_2	$k_1 = 4.36\ (0.12) \times 10^{-1}$, $R^2 = 0.99$	$V_m = 3.65\ (0.93) \times 10^2$, $K_s = 5.17\ (2.05) \times 10^2$, $R^2 = 1.00$
	GS-15	Acetate	$k_1 = 6.36\ (0.27) \times 10^{-2}$, $R^2 = 0.99$	$V_m = 4.37\ (1.07) \times 10^1$, $K_s = 3.92\ (1.63) \times 10^2$, $R^2 = 1.00$
Co(III)EDTA	BrY	Lactate	$k_1 = 1.13\ (0.10) \times 10^{-1}$, $R^2 = 0.96$	$V_m = 4.91\ (0.62) \times 10^1$, $K_s = 1.28\ (0.74) \times 10^2$, $R^2 = 0.99$
		H_2	$k_1 = 4.34\ (0.21) \times 10^{-1}$, $R^2 = 0.99$	$V_m = 5.90\ (2.76) \times 10^2$, $K_s = 5.81\ (4.18) \times 10^2$, $R^2 = 0.99$
	CN32	Lactate	$k_1 = 5.53\ (0.37) \times 10^{-2}$, $R^2 = 0.97$	$V_m = 1.99\ (0.13) \times 10^1$, $K_s = 4.59\ (1.94) \times 10^1$, $R^2 = 1.00$
		H_2	$k_1 = 2.24\ (0.07) \times 10^{-1}$, $R^2 = 0.99$	$V_m = 2.02\ (0.57) \times 10^2$, $K_s = 9.81\ (0.85) \times 10^2$, $R^2 = 0.99$
	MR-1	Lactate	$k_1 = 1.37\ (0.09) \times 10^{-1}$, $R^2 = 0.98$	$V_m = 6.04\ (1.15) \times 10^1$, $K_s = 1.30\ (0.79) \times 10^2$, $R^2 = 1.00$
		H_2	$k_1 = 2.91\ (0.11) \times 10^{-1}$, $R^2 = 0.99$	$V_m = 3.54\ (1.98) \times 10^2$, $K_s = 8.91\ (6.67) \times 10^2$, $R^2 = 0.99$
	GS-15	Acetate	$k_1 = 3.35\ (0.16) \times 10^{-2}$, $R^2 = 0.99$	$V_m = 1.72\ (0.14) \times 10^1$, $K_s = 2.39\ (0.41) \times 10^2$, $R^2 = 1.00$
UO_2^{2+}	BrY	Lactate	$k_1 = 1.43\ (0.08) \times 10^{-2}$, $R^2 = 0.99$	$V_m = 6.45\ (2.92)$, $K_s = 171\ (19.4)$, $R^2 = 1.00$
		H_2	$k_1 = 2.47\ (0.10) \times 10^{-2}$, $R^2 = 0.99$	$V_m = 16.9\ (2.00)$, $K_s = 423\ (78.6)$, $R^2 = 1.00$
	CN32	Lactate	$k_1 = 9.69\ (0.50) \times 10^{-3}$, $R^2 = 0.98$	$V_m = 4.86\ (1.74)$, $K_s = 209\ (73.8)$, $R^2 = 1.00$
		H_2	$k_1 = 1.17\ (0.04) \times 10^{-2}$, $R^2 = 0.99$	$V_m = 7.00\ (1.75)$, $K_s = 295\ (123)$, $R^2 = 1.00$
	MR-1	Lactate	$k_1 = 1.97\ (0.18) \times 10^{-2}$, $R^2 = 0.97$	$V_m = 6.66\ (0.89)$, $K_s = 53.9\ (21.6)$, $R^2 = 1.00$
		H_2	$k_1 = 1.99\ (0.14) \times 10^{-2}$, $R^2 = 0.98$	$V_m = 11.5\ (2.39)$, $K_s = 297\ (154)$, $R^2 = 1.00$
	GS-15	Acetate	$k_1 = 3.81\ (0.10) \times 10^{-3}$, $R^2 = 1.00$	$V_m = 2.25\ (0.61)$, $K_s = 274\ (158)$, $R^2 = 1.00$
CrO_4^{2-}	BrY	Lactate	$k_1 = 8.95\ (0.99) \times 10^{-3}$, $R_m = 306\ (14)$, $R^2 = 0.96$	$V_m = 1.97\ (11500) \times 10^4$, $K_s = 2.13\ (12{,}400) \times 10^6$, $R_m = 303\ (25)$, $R^2 = 0.96$
	CN32	Lactate	$k_1 = 8.41\ (0.41) \times 10^{-3}$, $R_m = 994\ (161)$, $R^2 = 1.00$	$V_m = 7.36\ (13.3)$, $K_s = 4.39\ (16.2) \times 10^2$, $R_m = 662\ (541)$, $R^2 = 1.00$
	MR-1	Lactate	$k_1 = 7.48\ (0.68) \times 10^{-3}$, $R_m = 480\ (39)$, $R^2 = 0.98$	$V_m = 1.50\ (12800) \times 10^4$, $K_s = 2.10\ (17{,}900) \times 10^6$, $R_m = 543\ (402)$, $R^2 = 0.98$
TcO_4^-	CN32	Lactate	$k_1 = 2.17\ (0.09) \times 10^{-4}$, $R^2 = 0.95$	$V_m = 7.11\ (191) \times 10^2$, $K_s = 5.32\ (145) \times 10^4$, $R^2 = 0.95$
		H_2	$k_1 = 1.51\ (0.12) \times 10^{-3}$, $R^2 = 0.96$	$V_m = 8.21\ (2.91) \times 10^1$, $K_s = 1.00\ (308)$, $R^2 = 0.96$

[a]Excess electron donor concentrations were used in all cases.

[b]Parameters have units: k_1 (min^{-1}) for first-order model: V_m (μM/min) and K_s (μM) for Monod model with no growth; R_m (μM). Numbers in parentheses were estimated standard deviation of the parameter estimate. The parameters were estimated by fitting the total concentration averaged for replicates versus time curves in Figs. 1–6. The total cell concentration in parameter estimation used a constant cell concentration $2.0(\pm 0.1) \times 10^8$ cells/mL (bracket is one standard deviation) for each data set.

the data. This large standard deviation was caused by the high correlation of the Monod parameters due to the model over-parametrization. Therefore, it is important to include estimation errors with the Monod parameters (Table II). The method used to estimate the standard deviations of the Monod parameters under growth and no growth conditions was reported previously (Liu and Zachara, 2001). In contrast, the uncertainties of the first-order coefficients were small (Table II). Because the first-order rate coefficient reflects a reduction rate normalized by the substrate concentration, it is better for comparison of metal reduction rates observed under different conditions. The first-order model could also simplify numerical calculations of biotransformation in the simulation of solute reactive transport in sediments and groundwater (Hunter et al., 1998).

Rates of Metal Reduction by DMRB

The metal reduction rates by the three *Shewanella* species when coupled to H_2 were nearly twice as fast as when lactate$^-$ was provided as an electron donor for all metals except CrO_4^{2-}. The higher reduction rate using H_2 was achieved despite its lower initial electron equivalent (0.96 mmol/L of e^-) than lactate (40 mmol/L of e^-) provided in all comparative experiments. The more rapid reduction when H_2 was used as an electron donor was consistent with other observations for Tc(VII) reduction using CN32 (Wildung et al., 2000) and sulfate-reducing bacteria (Lloyd et al., 2001). A slower rate of CrO_4^{2-} reduction using H_2 as electron donor as compared to lactate$^-$ was also reported for sulfate-reducing bacteria (Lloyd et al., 2001).

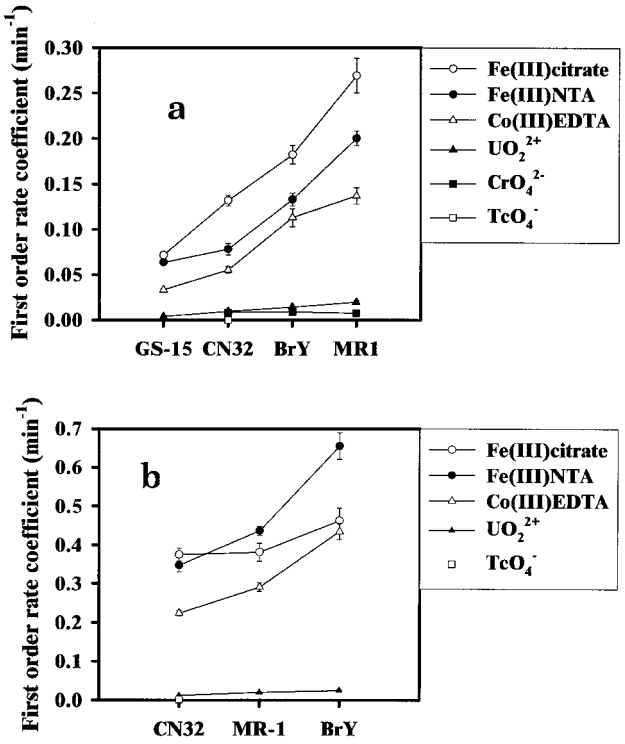

Figure 7. Observed trends in first-order rate coefficients for different metals and DMRB with lactate$^-$ (a) or H_2 (b) as electron donor.

Two plausible explanations may account for the more rapid bioreduction of all metals except CrO_4^{2-} with H_2. First, electrons generated by soluble or periplasm-associated H_2 hydrogenase may pass through the electron transport chain more rapidly than those generated from lactate dehydrogenase. Studies of sequential electron transport in a sulfate-reducing bacteria, *Desulfomicrobium norvegicum*, revealed that electrons liberated by a catalytic periplasmic Ni-Fe-S hydrogenase directly pass to tetraheme cytochrome c_3 (M_r 13,000) and then are distributed to octaheme cytochrome c_3 (M_r 26,000) and to subsequent components of the organism's electron transport chain (Aubert et al., 2000). The electron transport chain eventually directs electrons toward outer-membrane cytochromes that may function as a terminal metal reductase (Lojou et al., 1998; Lovley et al., 1993). Alternatively, electrons released from lactate dehydrogenase may have to travel more circuitous routes. PSORT analysis of the predicted amino acid sequence of the lactate dehydrogenase [derived from the preliminary genomic sequence provided by The Institute for Genomic Research website at http://www.tigr.org] suggests that this enzyme is located in the cell (inner) membrane whereas both the Fe and NiFe hydrogenases [also derived from the genome sequence] are predicted to reside in the periplasm (Margie Romine, personal communication). Additional steps, including intermediates such NADH, are required to conduct electrons released from lactate dehydrogenase into the electron transport chain (Brock et al., 1994). Second, the small size and neutral charge of H_2 could allow a faster diffusion rate or less energy to migrate to sites of enzymatic activity. The diffusion coefficient of H_2 is about 4.5×10^{-5} cm^2/s while that of lactate is about 9.5×10^{-6} cm^2/s in dilute solution (Cussler, 1995). The negative charge of the lactate ion could also inhibit its diffusion to the cell surface from solution. The mass flux of a charged

TABLE III. Overall reactions and free energy changes of metal reduction by DMRB.[a]

Reactions	$\Delta G_r^{o\prime}$	ΔG_r
$4FE(III)citrate + lactate^- + 2H_2O = 4Fe(II)citrate^- + acetate^- + HCO_3^- + 5H^+$	−70.90	−82.75
$4Fe(III)NTA + lactate^- 2H_2O = 4Fe(II)NTA^- + acetate^- + HCO_3^- + 5H^+$	−69.62	−81.47
$4Co(III)EDTA^- + lactate^- + 2H_2O = 4Co(II)EDTA^{2-} + acetate^- + HCO_3^- + 5H^+$	−69.51	−81.36
$2UO_2^{2+} + lactate^- + 2H_2O = 2UO_2 + acetate^- + HCO_3^- + 5H^+$	−80.61	−77.03
$(4/3)CrO_4^{2-} + lactate^- + (5/3)H^+ + (2/3)H = (4/3)Cr(OH)_3 + acetate^- + HCO_3^-$	−99.37	−98.72
$(4/3)TcO_4^- + lactate^- + (1/3)H^+ = (4/3)TcO_2 + acetate^- + HCO_3^- + (2/3)H_2O$	−68.01	−67.36
$2Fe(III)citrate + H_2 = 2Fe(II)citrate^- + 2H^+$	−69.89	−65.87
$2Fe(III)citrate + H_2 = 2Fe(II)NTA^- + 2H^+$	−68.61	−64.59
$2Co(III)EDTA^- + H_2 = 2Co(II)EDTA^{2-} + 2H^+$	−68.50	−64.48
$UO_2^{2+} + H_2 = UO_2 + 2H^+$	−79.60	−60.58
$(2/3)CrO_4^{2-} + H_2 + (4/3)H^+ = (2/3)Cr(OH)_3 + (2/3)H_2O$	−98.35	−82.51
$(2/3)TcO_4^- + H_2 + (2/3)H^+ = (2/3)TcO_2 + (4/3)H_2O$	−66.99	−51.15
$8Fe(III)citrate + acetate^- + 4H_2O = 8Fe(II)citrate^- + 2HCO_3^- + 9H^+$	−56.83	−63.11
$8Fe(III)NTA + acetate^- + 4H_2O = 8Fe(II)NTA^- + 2HCO_3^- + 9H^+$	−55.55	−61.83
$8Co(III)EDTA^- + acetate^- + 4H_2O = 8Co(II)EDTA^{2-} + 2HCO_3^- + 9H^+$	−55.44	−61.72
$4UO_2^{2+} + acetate^- + 4H_2O = 4UO_2 + 2HCO_3^- + 9H^+$	−66.54	−57.82
$(8/3)CrO_4^{2-} + acetate^- + (13/3)H^+ + (4/3)H_2O = (8/3)Cr(OH)_3 + 2HCO_3^-$	−85.30	−79.77
$(8/3)TcO_4^- + acetate^- + (5/3)H^+ + = (8/3)TcO_2 + 2HCO_3^- + (4/3)H_2O$	−53.94	−48.41

[a]Free energy changes in units of kJ/mol of electron transfer. $\Delta G_r^{o\prime}$: standard reaction free energy change corrected to pH 7; it was calculated using standard free energy of formation for lactate, acetate, citrate, carbonate species, H_2, Fe(II), Fe(III), H_2O from the compilation in Brock et al. (1994); Tc species from Rard et al. (1999); U species from Grenthe et al. (1992); and complexation or solubility constants for Fe(III)citrate, Fe(II)citrate, Fe(III)NTA, and Fe(II)NTA, Co(III)EDTA, Co(II)EDTA, $Cr(OH)_{3(c)}$, and H_2CrO_4 from Martell and Smith (2001). ΔG_r: the reaction free change. The values of ΔG_r in the table were calculated using $\Delta G_r^{o\prime}$ corrected by the concentrations of aqueous species when 10% of electron acceptor is reduced according to the stoichiometric relationship. The initial concentrations of electron acceptor = 0.5 m*M*, electron donor lactate$^-$ (or acetate) = 10 m*M*, H_2 = 0.48 mmol/L, and HCO_3^- = 26 m*M*. Activity corrections and aqueous complexes other than those involved in the listed reactions were not considered.

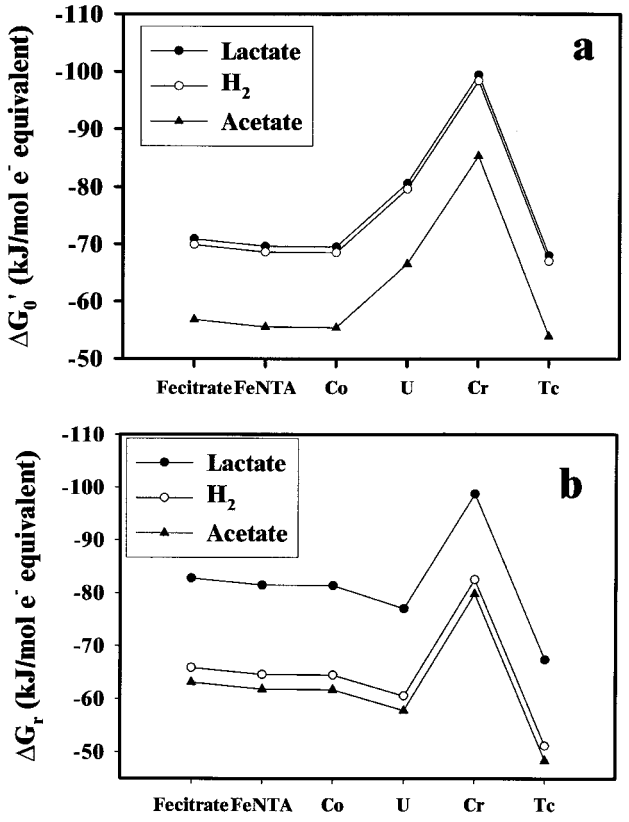

Figure 8. Overall reaction free energy change for metal reduction coupled with oxidation of lactate$^-$, H_2, and acetate$^-$ as electron donor. (a) Standard free energy change corrected to pH 7; (b) reaction free energy change at aqueous species concentrations in suspensions with 10% of electron acceptor reduced at pH 7 according to the stoichiometric relationship in Table III.

ion in a potential field is described by the Nerst–Planck equation (Bard and Faulkner, 1980):

$$\vec{J}_i = -(D_i \nabla C_i + \mu_i C_i Z_i \nabla \Psi), \quad (7)$$

where $\vec{J}_i$ is the vector of mass flux for a species i, D_i is the diffusion coefficient, C_i is the concentration, μ_i is the mobility (negative for negatively charged ions), Z_i is the charge, Ψ is the electrochemical potential, and ∇ is the gradient symbol. According to Eq. (7), in a negatively charged electrochemical field, such as on the bacterial surfaces (Sokolov et al., 2001; Van der Wal et al., 1997), the diffusion of a negatively charged ion driven by concentration gradient, ∇C_i, is retarded by the electrochemical force, $\nabla\Psi$. A negative electrochemical potential has no effect on the diffusion of neutral species and can increase the flux of positively charged ions. The location of lactate dehydrogenase in the cell membrane and negatively charged potential field on the bacterial surface will likely require an active transport system associated with the outer membrane and periplasm region. Thus, cells have to invest energy to overcome the exclusion force resulted from the interaction between the negatively charged lactate$^-$ and outer-membrane surface.

The reduction rates of the Fe(III) complexes were faster than Co(III)EDTA$^-$ that, in turn, were much faster than the reduction rates of $U(VI)O_2^{2+}$, $Cr(VI)O_4^{2-}$, and $Tc(VII)O_4^-$ (Fig. 7). After accounting for the number of electron transfers per mole of electron acceptor, the reduction rates of U(VI), Cr(VI), and Tc(VII) were still about one-half of

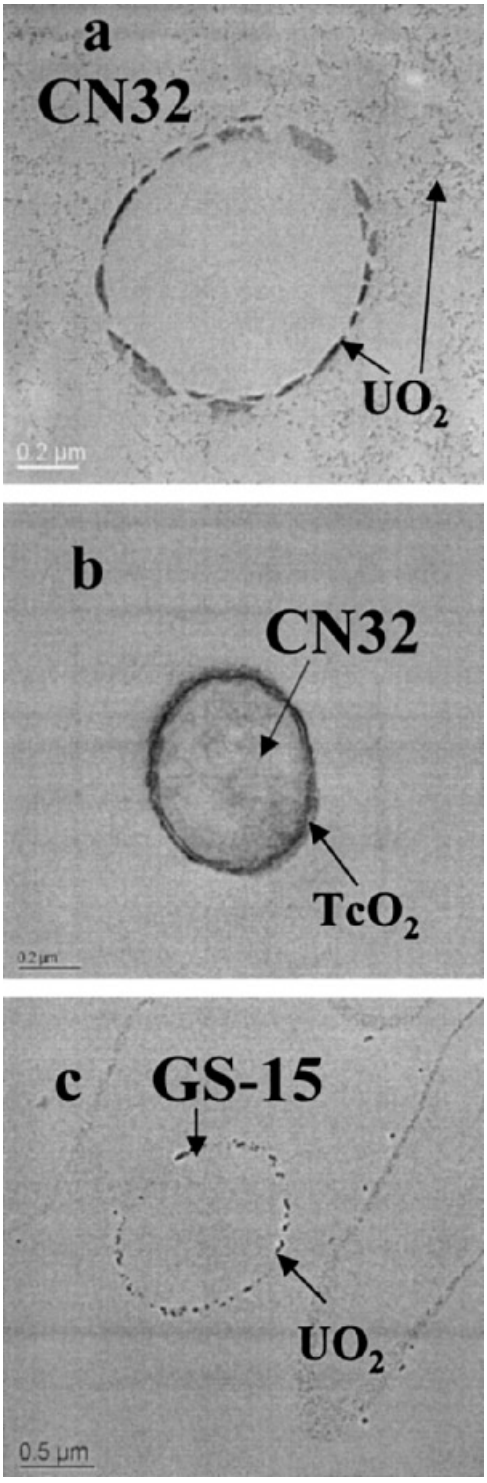

Figure 9. TEM images showing the distribution of precipitates on the bacterial surfaces and periplasmic space following the reduction of U(VI) by CN32 (a), Tc(VII) by CN32 (b), and U(VI) by GS-15 (c).

TABLE IV. Thermodynamic properties of some reduction products.

Metal	Reduction product form	Reaction constant	Solubility (μM)[a]
Fe(III)citrate	$Fe^{2+} + citrate^{3-} = Fe(II)citrate^{-}$	log K = 5.68[b]	
Fe-NTA	$Fe^{2+} + NTA^{3-} = Fe(II)NTA^{-}$	log K = 9.85[b]	
$CoEDTA^{-}$	$Co^{2+} + EDTA^{4-} = Co(II)EDTA^{2-}$	log K = 17.97[b]	
UO_2^{2+}	$U^{4+} + 2H_2O = UO_2 + 4H^{+}$	log K = 4.7[c]	$10^{-26.7}$ as U^{4+}
CrO_4^{2-}	$Cr^{3+} + 3H_2O = Cr(OH)_3 + 3H^{+}$	log K = −11.9[b]	$10^{-3.1}$ as Cr^{3+}
TcO_4^{-}	$TcO^{2+} + H_2O = TcO_2 + 2H^{+}$	log K = 8.56[d]	$10^{-22.6}$ as TcO^{2+}

[a]Solubility was calculated for pH 7.
[b]From Martell and Smith (2001).
[c]Calculated with standard free energy of formation from Grenthe et al. (1992).
[d]Calculated with standard free energy of formation from Rard et al. (1999).

those for $Co(III)EDTA^{-}$ and one-third of those of the Fe(III)-chelate complexes. Mass transport and physiologic effects may account for these differences. The dominant aqueous species of the metals studied were $Fe(III)citrate^0$, $Fe(III)NTA^0$, $Co(III)EDTA^{-}$, $UO_2(CO_3)_3^{4-}$, CrO_4^{2-}, and TcO_4^{-} in the bicarbonate buffer system. The aqueous species in the Fe(III)citrate system are not well known but may also include $Fe(III)Hcitrate^{+}$ and $Fe(III)H_2citrate^{2+}$ (Escoda et al., 1999). As shown by Eq. (7), the diffusive flux of negatively charged aqueous species into the outer membrane may be retarded by the electrochemical field. This mass transfer effect may account for the faster bioreduction rates of the Fe(III) complexes relative to the others. However, it is an inadequate explanation of the other trend, where, for example, solutes of like charge (e.g., $Tc(III)O_4^{-}$ and $Co(III)EDTA^{-}$) were bioreduced at different rates.

The polyvalent solutes that precipitated upon bioreduction were reduced more slowly than the others. The stable, lower valence states of Tc, U, and Cr, are sparingly soluble at circumneutral pH (Table III), and these products precipitated on and within the cells. The nanometer-sized precipitates may physically block the metal reductase(s) or intermediate electron transport sites, and/or reduce the porosity of bacterial membrane or transport channels for the electron donor or acceptor. The precipitates may also have general inhibitory effects on cell viability, vigor, or overall physiologic state. A recent study of Fe(III) reduction has shown that mineral precipitation on the cell surface could inhibit the Fe(III) reduction (Liu et al., 2001c). In contrast, the reduction products $Co(II)EDTA^{2-}$, $Fe(II)citrate^{-}$, and $Fe(II)NTA^{-}$ are probably released quickly from the outer-membrane region to bulk solution through concentration gradient and electrochemical forces.

Implications

Kinetic rates and models are required to evaluate the feasibility of microbial metal reduction as a technique of in-situ immobilization of contaminant metals and to design and control remediation systems in practical applications. The results of this study demonstrated that the kinetics of dissimilatory microbial reduction of metals followed the Monod-based kinetics, which have been widely used in the design and control of modern microbiological wastewater treatment systems (Rittmann and McCarty, 2001; Tchobanoglous and Burton, 1991). Although these treatment systems were primarily designed for treating organic contaminants (Rittmann and McCarty, 2001), the biotechnologies developed based on the Monod kinetic models may be adapted and applied to the systems of microbial metal reduction.

The trend of metal reduction rates observed in this study provides a potential sequence of metal reduction in a treatment system with mixed metals because a metal with a fast reduction rate should be kinetically more competitive for electrons from DMRB than one with a slower rate. The aqueous Fe(III) complexes, which showed the highest reduction rate in this study, may play as an inhibitory role to the reduction of contaminant metals Co, Tc, U, and Cr. However, this inhibitory effect should be minimal in many aqueous systems except those containing Fe(III) complex ligands because of the low solubility of Fe(III) species in circumneutral environments. The reduction rate of solid phase Fe(III) is slow relative to soluble complexes. For example, the first-order reduction rate of goethite by CN32 was about 4.5×10^{-4} min^{-1} (Liu et al., 2001a), which is 1 order of magnitude slower than those of soluble contaminant metals (Table II). The kinetic rates and sequence of metal reduction by DMRB in this study were affected by the strain of DMRB, type of electron donor, type of acceptor, and the properties and location of the reduction products. The kinetic rates were determined with electron acceptor as a rate-limiting variable, a scenario reflecting the stimulated metal reduction or natural environments with high content of organic matters so that electron donor is in excess. When electron donor is also a rate-limiting variable, the overall metal reduction rate will be a function of both electron acceptor and donor concentrations (Liu et al., 2001a). The abiotic redox interaction between bioreduction products and oxides may also significantly affect the overall metal reduction rates. Recent studies on the microbial reduction of U(VI) demonstrated that the reduction rate and extent were significantly decreased by the presence of Fe(III) oxides (Nevin and Lovley, 2000; Wielinga et al., 2000) and Mn

oxides (Fredrickson et al., 2001; Liu et al., 2001b). On the other hand, the presence of iron oxides increased the extent and rate of Cr(VI) reduction by BrY (Wielinga et al., 2001). The overall kinetic rates of metal reduction in these complex systems will be controlled by the coupling and interaction of individual microbial and abiotic processes (Liu et al., 2001b). The results from this study provide rates for the microbial reduction of individual metals that can provide the foundation for investigating coupled reactions.

Although the Monod expression fitted the macroscopic metal reduction results in this study quite well, the interpretation of metal reduction rate and rate trend requires fundamental understanding of the mechanisms for the mass transfer of electron donors, acceptors, and their products between enzyme locations and bulk solution and of membrane-associated electron transport from donors to acceptors. The complex electrochemical and biochemical structures of bacterial surfaces and membranes pose a significant challenge to rigorously analyze and model the mass transfer within the microenvironments of a bacterial cell. Involvement of various membrane-associated enzymes in the electron transport system from donor to acceptor also provides a formidable task to deconvolute the network of biochemical reactions controlling the flux of electrons. The studies in these two directions, however, would fundamentally improve the kinetic models and would provide better predictions of metal reduction and rate sequence.

Pacific Northwest National Laboratory is operated for DOE by Battelle Memorial Institute under Contract DE AC06-76 RLO 1830. We appreciate Dr. Margie Romine at PNNL for information regarding the location of lactate dehydrogenase for *S. oneidensis* MR-1 based on genome sequence and the Institute for Genomic Research for making preliminary data available from the genome sequence of *S. oneidensis* MR-1

References

Allison JD, Brown DS, Novo-Gradac KJ. 1991. MINITEQA2// PRODEFA2, A geochemical assessment model for environmental systems (version 3). Washington, D.C.: USEPA Environmental Research Laboratory. p 105.

Atlas RM. 1993. Microbial ecology: fundamentals and applications. San Francisco: Benjamin Cummings Publishing Co.

Aubert C, Brugna M, Dolla A, Bruschi M, Giudici-Orticoni M-T. 2000. A sequential electron transfer from hydrogenases to cytochromes in sulfate-reducing bacteria. Biochim Biophys Acta 1476:85–92.

Bae W, Rittmann BE. 1996. A structural model of dual-limitation kinetics. Biotechnol Bioeng 49:683–689.

Bard AJ, Faulkner LR. 1980. Electrochemical methods: fundamentals and applications. New York: Wiley.

Brock TD, Madigan MT, Martinko JM, Parker J. 1994. Biology of microorganisms. Englewood Cliffs, NJ: Prentice-Hall, Inc.

Caccavo FJ, Blakemore RP, Lovley DR. 1992. A hydrogen-oxidizing Fe(III) reducing microorganism from the Great Bay Estuary, New Hampshire. Appl Environ Microbiol 58:3211–3216.

Cussler EL. 1995. Diffusion: mass transfer in fluid systems. Cambridge, England: Cambridge University Press.

De Luca G, De Philip P, Dermoun Z, Rousset M, Vermeglio A. 2001. Reduction of Technetium(VII) by *Desulfovibrio fructosovorans* is mediated by the nickel–iron hydrogenase. Appl Environ Microbiol 67: 4583–4587.

Dwyer FP, Gyarfas EC, Mellor DP. 1955. The resolution and racemization of potassium ethylenediaminetetraacetateocobaltate (III). J Phys Chem 59:296–297.

Easterby JS. 1984. The kinetics of consecutive enzyme reactions. The design of coupled assays and the temporal response of pathways. Biochem J 219:843–847.

Easterby JS. 1989. The analysis of metabolite channelling in multienzyme complexes and multifunctional proteins. Biochem J 264:605–607.

Escoda ML, de la Torre F, Salvado V. 1999. The formation of mixed ligand complexes of Fe(III) with phosphoric and citric acids in 0.5 *M* $NaNO_3$ aqueous solutions. Polyhedron 18:3269–3274.

Fredrickson JK, Zachara JM, Kennedy DW, Liu C, Duff MC, Hunter DB, Dohnalkova A. 2001. Influence of Mn oxides on the reduction of U(VI) by the metal-reducing bacterium *Shewanella putrefaciens*. Geochim Cosmochim Acta (in press).

Gaudy AFJ, Gaudy ET. 1980. Microbiology for environmental scientists and engineers. New York: McGraw-Hill, Inc.

Gorby YA, Caccavo FJ, Bolton HJ. 1998. Microbial reduction of Co(III)EDTA in the presence and absence of manganese(IV) oxide. Environ Sci Technol 32:244–247.

Gorby YA, Lovley DR. 1992. Enzymatic uranium precipitation. Environ Sci Technol 26:205–207.

Grenthe I, Fuger J, Konings RJM, Lemire RJ, Muller AB, Nguyen-Trung C, Wanner H. 1992. Chemical thermodynamics. Vol. 1. Chemical thermodynamics of uranium. New York: OECD-NEA, Elsevier.

Hunter KS, Wang Y, Van Cappellen P. 1998. Kinetic modeling of microbially-derived redox chemistry of subsurface environments: coupling transport, microbial metabolism and geochemistry. J Hydrol 209: 53–80.

Jardine PM, Taylor DL. 1995. Kinetics and mechanisms of Co(II)EDTA oxidation by pyrolusite. Geochim Cosmochim Acta 59:4193–4203.

Liu C, Kota S, Zachara JM, Fredrickson JK, Brinkman C. 2001a. Kinetic analysis of the bacterial reduction of goethite. Environ Sci Technol 35:2482–2490.

Liu C, Zachara JM. 2001. Uncertainties of Monod parameters estimated from batch experiments. Environ Sci Technol 35:133–141.

Liu C, Zachara JM, Fredrickson JK, Kennedy DW, Dohnalkova A. 2001b. Modeling the inhibition of the bacterial reduction of U(VI) by β-$MnO_{2(s)}$. Environ Sci Technol 36:1452–1459.

Liu C, Zachara JM, Gorby YA, Szecsody JE, Brown CF. 2001c. Microbial reduction of Fe(III) and sorption/precipitation of Fe(II) on bacteria, *S. putrefaciens,* CN32. Environ Sci Technol 35:1385–1393.

Lloyd JR, Mabbett AN, Williams DR, Macaskie LE. 2001. Metal reduction by sulphate-reducing bacteria: physiological diversity and metal specificity. Hydrometallurgy 59:327–337.

Lloyd JR, Macaskie LE. 1996. A novel PhosphorImager-based technique for monitoring the microbial reduction of technetium. Appl Environ Microbiol 62:578–582.

Lojou E, Bianco P, Bruschi M. 1998. Kinetics studies of the electron transfer between bacterial *c*-type cytochromes and metal oxides. J Electroanal Chem 452:167–177.

Lovley DR. 1993. Dissimilatory metal reduction. Annu Rev Microbiol 47:263–290.

Lovley DR, Philips EJP. 1987. Rapid assay for microbially reducible ferric iron in aquatic sediments. Appl Environ Microbiol 523:1536–1540.

Lovley DR, Philips EJP. 1988. Novel mode of microbial energy metabolism: organic carbon oxidation coupled to dissimilatory reduction of iron or manganese. Appl Environ Microbiol 54:1472–1480.

Lovley DR, Phillips EJ, Gorby YA, Landa E. 1991. Microbial uranium reduction. Nature 350:413–416.

Lovley DR, Widman PK, Woodward JC, Phillips EJP. 1993. Reduction of uranium by cytochrome c_3 of *Desulfovibrio vulgaris*. Appl Environ Microbiol 59:3572–3576.

Martell AE, Smith RM. 2001. NIST critically selected stability constants of metal complexes database. Washington, DC: U.S. Department of Commence.

Monod J. 1949. The growth of bacterial cultures. Annu Rev Microbiol 3:371–393.

Moran F, Vlad MO, Ross J. 1997. Transition and transit time distribution for time dependent reactions with application to biochemical network. J Phys Chem B 101:9410–9419.

Myers CR, Nealson KH. 1988. Bacterial manganese reduction and growth with manganese oxide as the sole electron acceptor. Science 240: 1319–1321.

Myers CR, Nealson KH. 1990. Respiration-linked proton translocation coupled to anaerobic reduction of manganese(IV) and iron(III) in *Shewanella putrefaciens* Mr-1. J Bacteriol 172:6232–6238.

Nealson K, Saffarini D. 1994. Iron and manganese in anaerobic respiration: environmental significance, physiology, and regulation. Annu Rev Microbiol 48:311–343.

Nevin KP, Lovley DR. 2000. Potential for nonenzymatic reduction of Fe(III) via electron shuttling in subsurface sediments. Environ Sci Technol 34:2472–2478.

Rard JA, Rand MH, Anderegg G, Wanner H. 1999. Chemical thermodynamics. Vol 3. Chemical thermodynamics of technetium. New York: OECD-NEA, Elsevier Science.

Rittmann B, McCarty P. 2001. Environmental biotechnology: principles and applications. Columbus, OH: McGraw-Hill Higher Education.

Rittmann BE, VanBriesen JM. 1996. Microbiological processes in reactive modeling. Rev Mineral 34:311–334.

Robinson JA. 1985. Determining microbial kinetic parameters using nonlinear regression analysis: advantages and limitations in microbial ecology. Adv Microb Ecol 8:61–114.

Roden EE, Zachara JM. 1996. Microbial reduction of crystalline iron(III) oxides: influence of oxide surface area and potential for cell growth. Environ Sci Technol 30:1618–1628.

Roels JA. 1983. Energetics and kinetics in biotechnology. Amsterdam: Elsevier Biomedical Press BV.

Salvage KM, Yeh GT, Cheng HP, Cheng JR. 1996. Development of a model of subsurface hydrologic transport and biogeochemical reactions (HYDROBIOGEOCHEM). Comput Methods Water Resour XI: 517–524.

Segel IH. 1993. Enzyme kinetics: behavior and analysis of rapid equilibrium and steady-state enzyme systems. New York: John Wiley & Sons.

Simkins S, Alexander M. 1984. Models for mineralization kinetics with the variables of substrate concentration and population density. Appl Environ Microbiol 47:1299–1306.

Sokolov I, Smith DS, Henderson GS, Gorby YA, Ferris FG. 2001. Cell surface electrochemical heterogeneity of the Fe(III)-reducing bacteria *Shewanella putrefaciens*. Environ Sci Technol 35:341–347.

Spear JR, Figueroa LA, Honeyman BD. 1999. Modeling the removal of uranium U(VI) from aqueous solutions in the presence of sulfate-reducing bacteria. Environ Sci Technol 33:2667–2675.

Steefel CI, Van Cappellen P. 1998. Reactive transport modeling of natural systems. J Hydrol 209:1–7.

Tchobanoglous G, Burton FL. 1991. Wastewater engineering. New York: McGraw-Hill, Inc.

Tebes-Stevens C, Valocchi AJ, VanBriesen JM, Rittmann BE. 1998. Multicomponent transport with coupled geochemical and microbiological reactions: model description and example simulations. J Hydrol 209: 8–26.

Tribalat S, Beydon J. 1953. Isolement du technetium. Anal Chim Acta 8:22–28.

Van Cappellen P, Gaillard JF, Rabouille C. 1993. Biogeochemical transformations in sediments: kinetic models of early diagenesis. In: Wollast R, Mackenzie FT, and Chou L, editors. Interactions of C, N, P, and S biogeochemical cycles and global change. NATO ASI Series, Vol 14. Heidelberg: Springer-Verlag. p 401–445.

Van der Wal A, Norde AW, Zehnder AJB, Lyklema T. 1997. Conductivity and dielectric dispersion of Gram-positive bacterial cells. J Colloids Interface Sci 9:81–100.

Vlad MO, Moran F, Ross J. 1999. Transit time distribution of biochemical networks far from equilibrium: amplification of the probability of net transformation due to multiple reflections. J Phys Chem B 103:3965–3974.

Vlad MO, Ross J. 2000. Statistical ensemble approach and fluctuation-dissipation relations for multivariable chemical systems far from equilibrium. J Phys Chem A 104:3159–3176.

Wang Y-T, Shen H. 1997. Modeling Cr(VI) reduction by pure bacterial cultures. Water Res 31:727–732.

Wang Y-T, Xiao C. 1995. Factors affecting hexavalent chromium reduction in pure cultures of bacteria. Water Res 29:2467–2474.

Wielinga B, Bostick B, Hansel CM, Rosenzweig RF, Fendorf S. 2000. Inhibition of bacterially promoted uranium reduction: ferric (hydr)oxides as competitive electron acceptors. Environ Sci Technol 34:2190–2195.

Wielinga B, Mizuba MM, Hansel CM, Fendorf S. 2001. Iron-promoted reduction of chromate by dissimilatory iron-reducing bacteria. Environ Sci Technol 35:522–527.

Wildung RE, Gorby YA, Krupka KM, Hess NJ, Li SW, Plymale AE, McKinley JP, Fredrickson JK. 2000. Effect of electron donor and solution chemistry on products of dissimilatory reduction of technetium by *Shewanella putrefaciens*. Appl Environ Microbiol 66: 2451–2460.